DOI: 10.1002/anie.200704182

C_{60} Structures

Highly Selective Synthesis of C_{60} Disks on Graphite Substrate by a Vapor–Solid Process**

*Hyeon Suk Shin, Seok Min Yoon, Qun Tang, Bongwhan Chon, Taiha Joo, and Hee Cheul Choi**

Fullerene (C_{60}) is a potential component for organic transistors,[1] superconductors,[2] and optical switching devices.[3] Because these applications are based on the use of sets of specific electronic energy levels that would be determined by the mode of the geometrical assemblies of C_{60}, the development of synthetic methods for well-defined one-dimensional (1D) and 2D single crystals of C_{60} has been considered a key prerequisite.

Various 1D structures of C_{60} have been investigated because of practical advantages in device fabrication as well as the inherent interest in new architectures that might show unprecedented properties. Wirelike 1D structures have been synthesized directly on a solid substrate by a solvent-evaporation process and by spontaneous growth at the interface of immiscible solvents. Several types of 1D C_{60} nanostructures grown by these methods include nanowhiskers,[4] nanorods,[5] and nanotubes,[6] of which only nanorods have been reported to be single crystalline. In contrast, there are few reports of 2D structures of single-crystalline C_{60}. More importantly, the above-mentioned solution-based synthetic processes always include solvent molecules in the final structures. Solvent-free 1D or 2D C_{60} nanostructures can be synthesized by vapor-driven processes. Recently, 2D hexagonal-shaped C_{60} disks synthesized by a vapor-evaporation method were reported by Bao et al., but they were formed unselectively along with randomly grown 3D crystals.[1a] Herein we report a successful application of vapor–solid (VS) process for the highly selective synthesis of disk-shaped 2D single-crystalline C_{60}. We describe: 1) the substrate effect on the highly selective formation of C_{60} disks, 2) the structural characterization of the disks, 3) photoluminescence (PL) properties of the disks, and 4) the photoconductivity of a single disk.

The C_{60} disks were synthesized by a VS process.[7] Sublimed C_{60} powder (Aldrich, 99.9%) was placed in the middle of a quartz tube in a horizontal tube furnace, and a highly oriented pyrolytic graphite (HOPG) substrate supported on Si wafer was located near the end zone of the furnace (see Figure S1 in Supporting Information).

The shape of the C_{60} crystals proved to depend on the temperature of the tube furnace, the flow rate of the Ar carrier gas, the type of solid substrate, and the position of the substrate in the tube. Under optimum conditions (650 °C, 100 sccm of Ar (sccm = standard cubic centimeter per minute)), C_{60} disks were formed on HOPG (Figure 1a) with more than 50% surface coverage. Disks of several different shapes were observed, and two representative disks are shown in Figure 1b; one is a symmetric hexagonal-shaped disk and the other is an asymmetric one. It is noted that the area adjacent to the disks in Figure 1a was covered with a thin film. At a high Ar flow rate (1000 sccm) and a fixed reaction temperature, no disks were found; instead thin films predominantly formed (Figure 1c). It should be noted that the formation of disks is critically affected by the type of substrate. While C_{60} disks are predominantly produced on HOPG surface, only a few disks are randomly found on Si or

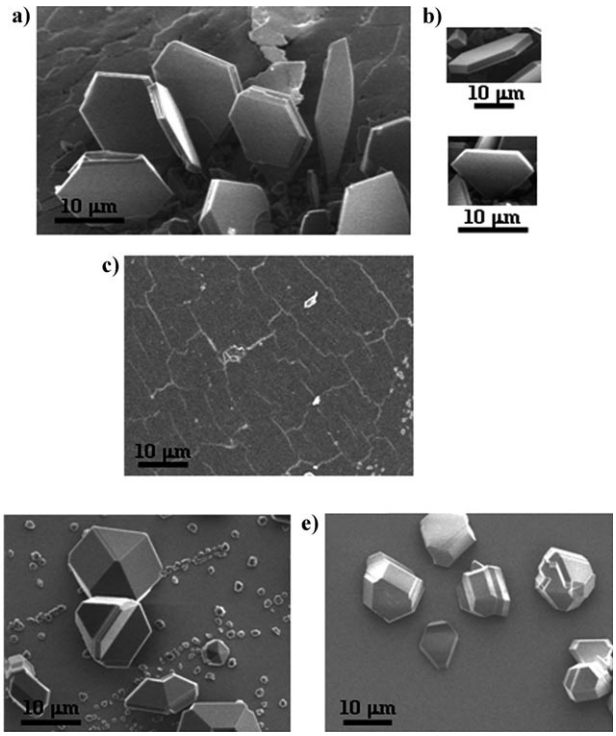

Figure 1. SEM images of disks (a and b) and films (c) on HOPG and 3D crystals on Si (d) and SiO_2 (e) wafers.

[*] Dr. H. S. Shin,[+] S. M. Yoon,[+] Dr. Q. Tang, B. Chon, Prof. T. Joo, Prof. H. C. Choi
Department of Chemistry
Pohang University of Science and Technology
San 31, Hyoja-dong, Pohang 790-784 (Korea)
Fax: (+82) 54-279-3399
E-mail: choihc@postech.edu
Homepage: http://www.postech.ac.kr/chem/nmrl

[+] H.S.S. and S.M.Y. have contributed equally to this work.

[**] This work was supported by the Nano/Bio Science & Technology Program of MOST (2006-00955), SRC/ERC Program (R11-2000-070-070020), Korean Research Foundation (MOEHRD; KRF-2005-005-J13103), and KOSEF (2007-8-1158).

Supporting information for this article is available on the WWW under http://www.angewandte.org or from the author.

SiO_2 wafers and mainly irregularly shaped 3D microcrystals are produced (Figure 1 d,e).

Since C_{60} is known to be easily polymerized upon application of external energy sources, such as electron beams or photons,[8] we characterized the C_{60} disks by measuring Raman spectra in order to determine if the disks and thin films in Figure 1 a,c consist of monomeric or polymeric C_{60}. Raman spectra measured for all disks and films show bands at the same wavenumber (1469 cm^{-1}) corresponding to A_g pentagonal pinch modes; this indicates that both the disks and the film retain pristine monomeric C_{60} molecules (Figure 2).

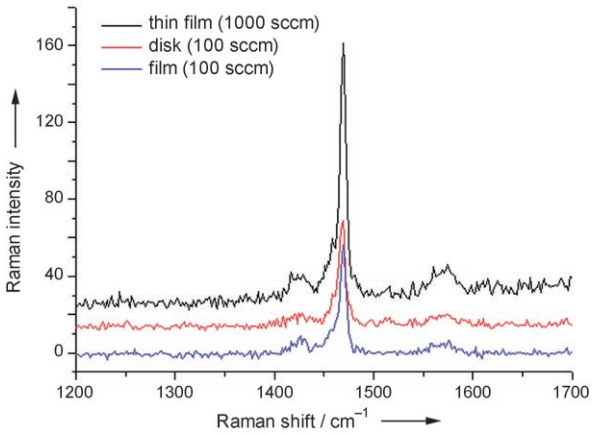

Figure 2. Raman spectra of a single C_{60} disk and the film in Figure 1 a (produced at 650 °C, 100 sccm of Ar) and the film in Figure 1 c (produced at 650 °C, 1000 sccm of Ar).

For the structural characterization, powder X-ray diffraction (XRD) spectra were obtained with the same samples that had been used for SEM in Figure 1. The red and blue spectra in Figure 3 a show XRD patterns of the disks (the sample in Figure 1 a) and the film (the sample in Figure 1 c), respectively. The XRD pattern of the disks supports a faced-centered cubic (fcc) structure (space group: *Fm*3*m* (225), JCPDS 85-1799), in which the four peaks are indexed as (111), (220), (311), and (222) from the fcc lattices.

Next, we characterized the C_{60} disks by high-resolution transmission electron microscopy (HRTEM) and confirmed that the crystal structures of the symmetric hexagonal-shaped disks and those of the asymmetric ones are identical. Figure 3 b shows a normal TEM image, a lattice image of HRTEM, and a fast Fourier transform (FFT) pattern of the symmetric hexagonal-shaped disk. The FFT pattern from a single C_{60} disk was obtained with respect to the [111] zone axis of fcc C_{60}. The resulting perspective view of a disk is shown in Figure 3 d. Figure 3 c exhibits a normal TEM image, a lattice image of HRTEM, and a FFT pattern of an asymmetric hexagonal-shaped disk. The FFT patterns of the symmetric and asymmetric disks indicate that the ratio of L_1 and L_2 as well as the crystal faces are identical. Thus, we believe that the two disks have the same fcc structures in their single crystals even though their morphologies are slightly different.

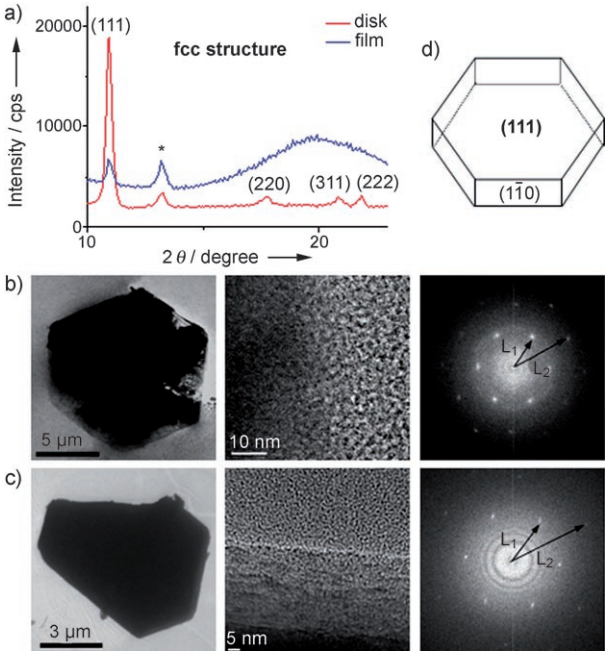

Figure 3. XRD spectra of C_{60} disks (red) and films (blue) (a), TEM and HRTEM images and a FFT pattern of a symmetric hexagonal-shaped disk (b) and of an asymmetric hexagonal-shaped disk (c), and perspective view of the hexagonal-shaped disk (d). The asterisk in (a) indicates the peak from HOPG.

The preferred growth of C_{60} disks on a HOPG substrate can be explained by the accepted theory on the determination of product morphology in VS processes. It is generally accepted that a low supersaturation ratio leads to the growth of 1D structures such as nanowhiskers and nanowires, while a high supersaturation ratio induces two-dimensional growth or the formation of isotropic bulk crystals.[7] For example, Lu et al. have shown that various-shaped crystals of Sn such as 1D nanowires, 2D nanosquares, 3D nanodisks, and isotropic particles can be grown by regulating the deposition temperature of the substrate.[7d,e] They monitored the change of the crystal shape depending on the deposition temperature by changing the supersaturation ratio, which was found to increase rapidly with decreasing deposition temperature. Under our experimental conditions, 3D crystal growth on Si or SiO_2 substrates indicates that the supersaturation ratio is high. On the other hand, a low supersaturation ratio is obtained when HOPG is used as the substrate instead of Si or SiO_2 under the same experimental conditions. The reasoning behind this substrate dependence is as follows: a thin film of C_{60} is first formed as a result of π–π interactions between C_{60} and HOPG, hence the actual vapor pressure of C_{60} on exposed HOPG must be lower than that on Si or SiO_2. The decreased vapor pressure results in a decrease of the supersaturation ratio, α ($\alpha = P/P_o$, where P is the actual vapor pressure and P_o is the equilibrium vapor pressure corresponding to the temperature).[7f,g] Indeed, the formation of the C_{60} thin film on HOPG is observed, and more importantly, C_{60} disks grow only on top of the C_{60} film (see Figure S2 in the Supporting Information). The preferred direction of 2D crystal growth is

the {1$\bar{1}$0} plane (Figure 3d). The {1$\bar{1}$0} plane is thermodynamically more unstable than the (111) plane, which has the lowest surface energy in fcc C_{60}.[8] Thus, the growth rate along the {1$\bar{1}$0} planes is faster, and finally the disk-shaped crystal results.

Further structural information on C_{60} disks was obtained from their photoluminescence (PL) spectra, which are sensitive to morphologies and defects in C_{60} crystals.[9,10] Figure 4a shows PL spectra of C_{60} powder, thin films, and

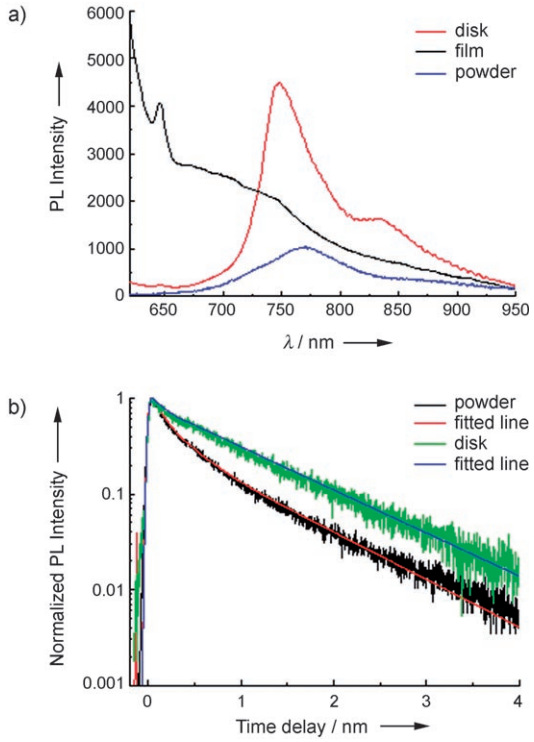

Figure 4. a) Photoluminescence (PL) spectra of C_{60} disks (red), films (black), and powder (blue). The PL intensity of the powder was multiplied 50 times. b) Time-resolved PL spectra of C_{60} disks (green) and powder (black). The fitting results show two components with different lifetimes from disks (red) and powder (blue), respectively.

disks. While high PL intensities were observed from the disks, negligible PL intensities were detected from thin films and powders. This is consistent with previous results, in which the emission strengths displayed by C_{60} crystal rods are higher than those of films.[5b] Compared to the PL spectrum of the powder, the PL bands of the disks were shifted to shorter wavelengths. Note that the main band at 748 nm can be assigned to the radiative transition from S_1 ($^1F_{1g}$) to S_0 (^1A_g).[8,10a] Although the reason for this blue shift is not clearly understood, the possibility of C_{60} polymerization in the disks can be safely excluded because this would induce a significant red shift of the PL band.[5b,10a] Meanwhile, the large increase in the PL intensity of the disks may result from the high crystallinity of C_{60} disk, which minimizes defects and torsional motions and hence suppresses nonradiative decay of the excited states.[11] The time-resolved PL (TRPL) for the band near 748 nm supports such a scenario. The TRPL of both disk and powder showed biexponential decay with the time constants of 150 ps (34%) and 970 ps (66%) for the disk, and 180 ps (72%) and 880 ps (28%) for the powder (Figure 4b). Although the time constants are similar, the smaller amplitude of the fast-decay component in the TRPL of the disk signifies less probability for the nonradiative decay owing to the higher crystallinity in the disk compared to the powder, resulting in higher PL intensity.

As one of the promising applications of C_{60} materials in optical devices, the photoconductivity of the C_{60} disks was measured. A single disk was removed from the substrate then transferred to prepatterned gold electrodes having a gap of 4 μm (inset of Figure 5). When the disk was irradiated with

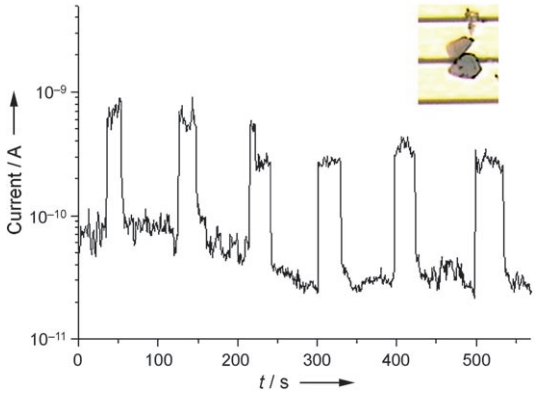

Figure 5. Photocurrent of a single C_{60} disk on a prepatterned gold electrode. A picture of the device is shown in the inset.

white light from a quartz halogen lamp, the current increased almost 10 times at a constant bias voltage of 30 V. To monitor the turn-on/off behavior, the irradiation was switched on and off more than 10 times without significant signal degradation, which is proof of the high reproducibility and reliability of the photoresponse (Figure 5). We further expect that much larger changes in photocurrent would be possible if the contact resistance at the interface between metal electrode and C_{60} disk is lowered by modification of the device as it has top-electrode configuration.

In summary, we have selectively prepared C_{60} disks on a HOPG substrate by a VS process. The C_{60} disks are single crystals having fcc structure and they show PL spectra with intensities higher than those of C_{60} films and powders. The photoconductivity of a single C_{60} disk points to possible applications in solar cells, optical switches, and photodetectors. We are currently fabricating C_{60} disk transistor devices to explore the electronic and magnetic properties of C_{60} disks.

Experimental Section

Synthesis of C_{60} disks: Sublimed C_{60} powder (Aldrich, 99.9%) was placed on the middle of horizontal quartz tube and an HOPG-coated Si, Si, or SiO_2 substrate was located at the end region of the tube. The temperature was increased up to 650 °C under a steady flow of Ar gas (100 or 1000 sccm) and was held for 30 min.

Characterization of C_{60} disks: The morphologies and the crystal structures of the C_{60} disks and films were characterized with a scanning electron microscope (SEM, XL30S, FEI), a high-resolution transmission electron microscope (HRTEM, JSM-6700F, JEOL), and

an X-ray diffractometer (XRD, D/MAX-1400 with K_α X-ray source, $\lambda = 0.15405$ nm, Rigaku). A photoluminescence (PL) measurement system consists of a home-built femtosecond optical parametric oscillator (OPO) and a time-correlated single-photon-counting (TCSPC) system. A frequency-doubled OPO laser (590 nm) was used as an excitation source. A TE-cooled CCD (Andor) detector and a microchannel plate photomultiplier tube (MCP-PMT) with a 30-cm monochromator (SP-300, Acton) were used for the PL and the time-resolved PL measurements. Raman spectra were measured with a Renishaw Raman system 3000 using an Ar ion laser (514.5 nm) as an excitation source.

Photoconductivity measurements: Current was measured by semiconductor analyzer (KEITHLEY 4200) with and without white-light irradiation using a quartz halogen lamp (Fiber-Lite Model 190, 30 W, Dolan-Jenner).

Received: September 11, 2007
Published online: December 11, 2007

Keywords: chemical vapor deposition · fullerenes · luminescence · photoconductivity

[1] a) A. L. Briseno, S. C. B. Mannsfeld, M. M. Ling, S. Liu, R. J. Tseng, C. Reese, M. E. Roberts, Y. Yang, F. Wudl, Z. Bao, *Nature* **2006**, *444*, 913; b) K. Itaka, M. Yamashiro, J. Yamaguchi, M. Haemori, S. Yaginuma, Y. Matsumoto, M. Kondo, H. Koinuma, *Adv. Mater.* **2006**, *18*, 1713; c) N. Takahashi, A. Maeda, K. Uno, E. Shikoh, Y. Yamamoto, H. Hori, *Appl. Phys. Lett.* **2007**, *90*, 083503; d) C. D. Dimitrakopoulos, P. R. Malenfant, *Adv. Mater.* **2002**, *14*, 99; e) R. C. Haddon, A. S. Perel, R. C. Morris, T. T. M. Palstra, A. F. Hebard, R. M. Fleming, *Appl. Phys. Lett.* **1995**, *67*, 121.

[2] a) A. R. Kortan, N. Kopylov, S. Glarum, E. M. Gyorgy, A. Ramirez, R. M. Fleming, F. A. Thiel, R. C. Haddon, *Nature* **1992**, *355*, 529; b) P. W. Stephens, L. Mihaly, P. L. Lee, R. L. Whetten, S.-M. Huang, R. Kaner, F. Deiderich, K. Holczer, *Nature* **1991**, *351*, 632.

[3] a) Y. J. Xing, G. Y. Jing, J. Xu, D. P. Yu, *Appl. Phys. Lett.* **2005**, *87*, 263117; b) J. Mort, M. Machonkin, R. Ziolo, D. R. Huffman, M. I. Ferguson, *Appl. Phys. Lett.* **1992**, *60*, 1735.

[4] a) J. Minato, K. Miyazawa, *Carbon* **2005**, *43*, 2837; b) K. Miyazawa, Y. Kuwasaki, A. Obayashi, K. Kuwabara, *J. Mater. Res.* **2002**, *17*, 83.

[5] a) L. Wang, B. Liu, D. Liu, M. Yao, Y. Hou, S. Yu, T. Cui, D. Li, G. Zou, A. Iwasiewicz, B. Sundqvist, *Adv. Mater.* **2006**, *18*, 1883; b) Y. Jin, R. J. Curry, J. Sloan, R. A. Hatton, L. C. Chong, N. Blanchard, V. Stolojan, H. W. Kroto, S. R. P. Silva, *J. Mater. Chem.* **2006**, *16*, 3715.

[6] a) H. Liu, Y. Li, L. Jiang, H. Luo, S. Xiao, H. Fang, H. Li, D. Zhu, D. Yu, J. Xu, B. Xiang, *J. Am. Chem. Soc.* **2002**, *124*, 13370; b) F. Tao, Y. Liang, G. Yin, D. Xu, Z. Jiang, H. Li, M. Han, Y. Song, Z. Xie, Z. Xue, J. Zhu, Z. Xu, L. Zheng, X. Wei, Y. Ni, *Adv. Funct. Mater.* **2007**, *17*, 1124; c) J. Minato, K. Miyazwa, *J. Mater. Res.* **2006**, *21*, 529.

[7] a) Z. W. Pan, Z. R. Dia, Z. L. Wang, *Science* **2001**, *291*, 1947; b) Z. R. Dai, Z. W. Pan, Z. L. Wang, *Adv. Funct. Mater.* **2003**, *13*, 9; c) Y. Xia, P. Yang, Y. Sun, Y. Wu, B. Mayers, B. Gates, Y. Yin, F. Kim, H. Yan, *Adv. Mater.* **2003**, *15*, 353; d) Y. Hsu, S. Lu, *J. Phys. Chem. B* **2005**, *109*, 4398; e) Y. Hsu, S. Lu, Y Lin, *Small* **2006**, *2*, 268; f) G. W. Sears, *Acta Metall.* **1955**, *3*, 361; g) G. W. Sears, *Acta Metall.* **1955**, *3*, 367.

[8] a) J. Yao, Y. Zou, X. Zhang, G. Chen, *Thin Solid Films* **1997**, *305*, 22; b) S. G. Wang, E. K. Tian, C. W. Lung, *J. Phys. Chem. Solids* **2000**, *61*, 1295; c) J. Zhang, F. Ma, K. Xu, *Appl. Surf. Sci.* **2004**, *229*, 34.

[9] M. S. Dresselhaus, G. Dresselhaus, P. C. Eklund in *Science of Fullerenes and Carbon Nanotubes*, Academic Press, San Diego, **1996**.

[10] a) Y. Wang, J. M. Holden, A. M. Rao, P. C. Eklund, U. D. Venkateswaran, D. Eastwood, R. L. Lidberg, G. Dresselhaus, M. S. Dresselhaus, *Phys. Rev. B* **1995**, *51*, 4547; b) T. L. Makarova, *Semiconductors* **2001**, *35*, 243.

[11] J. A. Riddle, S. P. Lathrop, J. C. Bollinger, D. Lee, *J. Am. Chem. Soc.* **2006**, *128*, 10986.

